Functional porous structures based on the pyrolysis of cured templates of block copolymer and phenolic resin

Kosonen, H; Valkama, S; Nykanen, A; Toivanen, M; ten Brinke, G; Ruokolainen, J; Ikkala, O; Nykänen, Antti

Published in:
Advanced materials

DOI:
10.1002/adma.200401110

DOI: 10.1002/adma.200401110

Functional Porous Structures Based on the Pyrolysis of Cured Templates of Block Copolymer and Phenolic Resin**

By *Harri Kosonen*,* *Sami Valkama*, *Antti Nykänen*, *Miika Toivanen*, *Gerrit ten Brinke*, *Janne Ruokolainen*, and *Olli Ikkala*

Porous materials with controlled pore sizes have been investigated for different applications such as filters, separation, sensors, supports for catalysis, and controlled drug release. Proper selection of chemical groups lining the pore walls, as well as detailed control of the pore size and size distribution, can lead to selectivity and various functions. In this work we describe a facile method to construct porous films by cross-linking phenolic resin in the presence of a self-assembled block-copolymer template, followed by pyrolysis at moderate temperature. This enables us to transfer the ordered block copolymer self-assembly into porosity, with a fine control of the pore size and distribution. These materials have large surface area (in excess of 300 $m^2 g^{-1}$), with a high number of phenolic hydroxyl groups at the matrix and pore walls, which can be used for, e.g., selective absorption or for further functionalization.

Concepts to prepare materials ranging from nanoporous (pores < 2 nm) or mesoporous (< 50 nm) up to macroporous (> 50 nm) have been previously demonstrated.[1–37] Typically, nanoporous materials are crystalline framework solids, such as zeolites, discotic molecular assemblies,[31–33] or "robust" molecular crystals formed using supramolecular[38] design principles.[2,11–20] These materials can have large void volumes and high internal surface areas, but the supramolecular materials often tend to collapse upon emptying the pores. Several approaches have also been presented to prepare mesoporous and macroporous materials, such as "track-etching",[4–6] using honeycomb structures,[27–29] and emptying nanostructured templates (e.g., sol–gel processing of surfactants or block copolymers,[7–10] selective degradation of material with UV exposure,[24–26] pyrolysis,[21–23,34] and selective removal of low-molecular-weight amphiphiles (combs) from hierarchically self-assembled polymeric comb–coil supramolecules[35,36]).

Block copolymers provide ideal structures for templates, as, by a facile route, they self-assemble into various structures as a result of the repulsion between the covalently bonded blocks; examples include the spherical, cylindrical, lamellar, and gyroid structures.[39–41] Previously, we have shown that alkylphenols can be selectively hydrogen-bonded to the pyridine groups of poly(styrene)-*block*-poly(4-vinylpyridine) (PS-*block*-P4VP) leading to hierarchical structures.[42,43] In addition, self-assembly is achieved upon mixing uncured phenolic resins and block copolymers consisting of a block that forms strong enough hydrogen bonds with the phenolic hydroxyls, and we have shown that in such cases the phenolic resin can be cured while the self-assembly is preserved.[44,45]

PS-*block*-P4VP copolymer (number-average molecular weights: $M_{n,PS} = 40\,000$ g mol^{-1} and $M_{n,P4VP} = 5600$ g mol^{-1}) was used to prepare mixtures with phenolic resin (Vulcadur RB, Bayer Ltd.) and the curing agent hexamethylenetetramine (HMTA); see Figure 1a for the structures. Owing to the hydrogen bonding between the pyridine and the phenolic resin,[45] self-assembled structures consisting of PS and P4VP/phenolic resin domains are formed (Fig. 1b). The relative weight fractions of the domains can be tuned to obtain different morphologies. After thermal curing at 100–190 °C, the aim was to selectively remove the PS-*block*-P4VP template using controlled pyrolysis (see Fig. 1c). Proper pyrolysis conditions were determined using the results of thermogravimetric analysis (TGA) (Fig. 2). Slow heating was used in order to minimize structural deformations of the films when the block-copolymer part was removed. Based on the TGA measurements, $T = 420$ °C was chosen to be the highest pyrolysis temperature, because, at that temperature, most of the block copolymer has been degraded whereas the weight of the cured phenolic matrix has not decreased significantly.

The structures of the cured and pyrolyzed complexes were analyzed using transmission electron microscopy (TEM) and small-angle X-ray scattering (SAXS). Figures 3a–f present TEM images of cured samples of different composition before and after pyrolysis. A "worm-like" structure with a periodicity of ca. 50 nm was observed for the materials before (Fig. 3a) and after pyrolysis (Fig. 3b) when the weight fraction of PS was $w_{PS} = 30$ %. Note that no staining was needed and the contrast after pyrolysis was significantly higher than before, which can be explained by the increased electron-density contrast between the domains upon pyrolytic removal of the block copolymer. A cylindrical morphology was observed when the weight fraction of PS was increased to $w_{PS} = 40$ % (Fig. 3c before and Fig. 3d after pyrolysis). The periodicity of the structure was ca. 50 nm and the diameter of the cylinders

[*] Dr. H. Kosonen, S. Valkama, A. Nykänen, M. Toivanen, Dr. J. Ruokolainen, Prof. O. Ikkala
Department of Engineering Physics and Mathematics and Center for New Materials, Helsinki University of Technology
P.O. Box 2200, FI-02015 HUT, Espoo (Finland)
E-mail: hkosonen@focus.hut.fi
Prof. G. ten Brinke
Materials Science Center, Dutch Polymer Institute
University of Groningen
Nijenborgh 4, NL-9747 AG Groningen (The Netherlands)

[**] M.Sc. Kati Vilonen, M.Sc. Jaakko Saarinen, and Lic.Sc. Jani Päivä-saari of Helsinki University of Technology are acknowledged for experimental assistance. This work was carried out in the Centre of Excellence of Academy of Finland ("Bio- and Nanopolymers Research Group", 77317). Beamtime on the BM26B (DUBBLE) has kindly been made available by The Netherlands Organization for Scientific Research (NWO) and we acknowledge Igor Dolbnya for experimental assistance and discussions.

ADVANCED MATERIALS

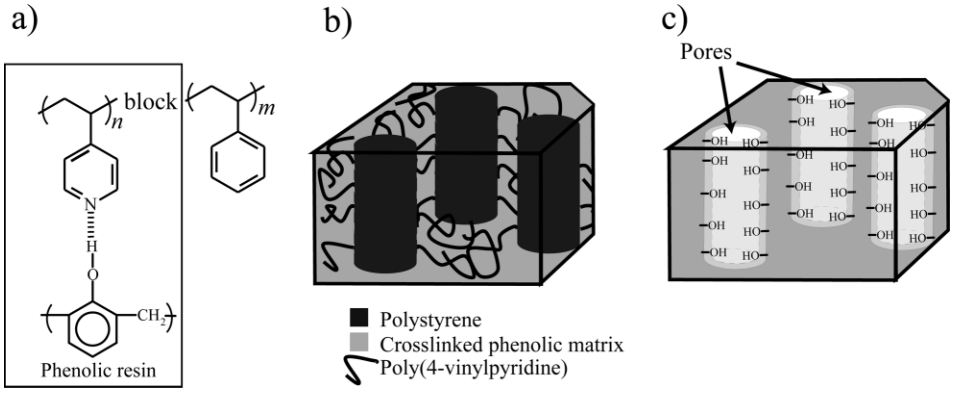

Figure 1. a) Phenolic resin, PS-*block*-P4VP and schematics of their mutual hydrogen bonding. b) As a result of hydrogen bonding, the phenolic resin and P4VP are confined within the same self-assembled domains as they microphase separate from the non-polar PS domains. Crosslinking at elevated temperatures "locks" the structure. c) During the selected pyrolysis conditions, PS-*block*-P4VP is essentially removed, leaving porous material with a narrow distribution of pore sizes, high surface area per volume unit, and hydroxyl groups at the porous matrix and the pore walls.

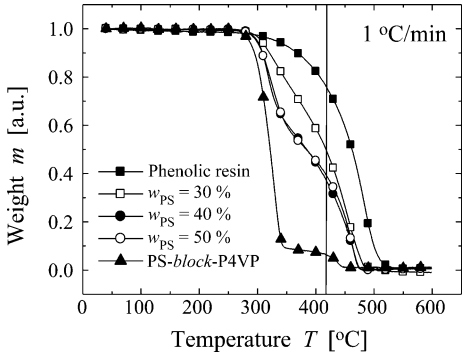

Figure 2. TGA curves for three HMTA-cured complexes of PS-*block*-P4VP/Phenolic resin ($M_{n,PS} = 40\,000$ g mol^{-1} and $M_{n,P4VP} = 5600$ g mol^{-1}) and reference materials (cured phenolic resin and PS-*block*-P4VP) under ambient atmosphere. The weight fraction of PS [w_{PS}] and the selected pyrolysis temperature 420 °C are indicated.

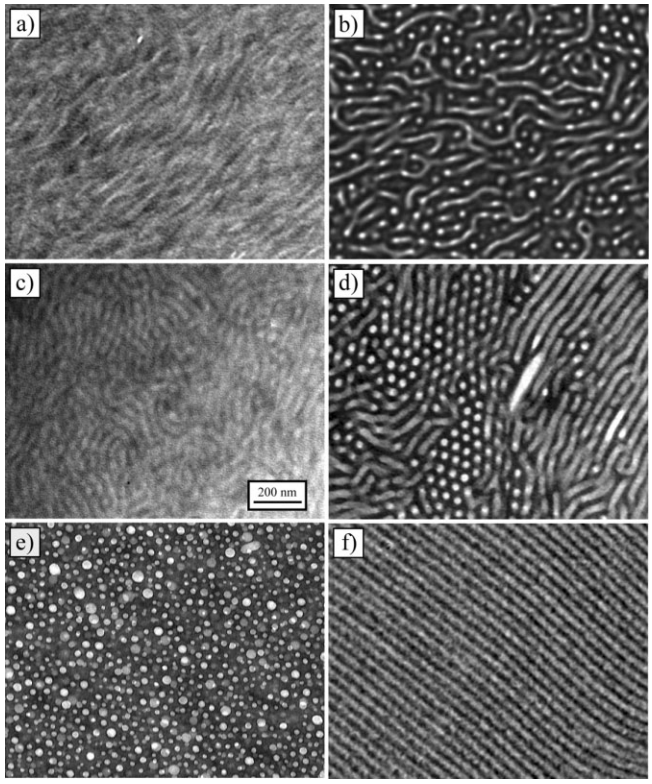

Figure 3. TEM images of HMTA-cured complexes of phenolic resin and PS-*block*-P4VP Samples were as follows: a) $w_{PS} = 30$ % before pyrolysis, b) $w_{PS} = 30$ % after pyrolysis, c) $w_{PS} = 40$ % before pyrolysis, d) $w_{PS} = 40$ % after pyrolysis, e) $w_{PS} = 20$ % after pyrolysis, and f) $w_{PS} = 60$ % before pyrolysis. The scale bar is indicated in (c) and is the same for all images.

was ca. 30 nm. Also, other morphologies can be obtained after curing, such as spherical (Fig. 3e, $w_{PS} = 20$ %, after pyrolysis) and lamellar (Fig. 3f, $w_{PS} = 60$ %, long period (L_p) = 42 nm, before pyrolysis). The spherical structure turned out to be more difficult to empty, because the degraded block-copolymer residues need to diffuse through the phenolic matrix. The lamellar structures, in turn, were difficult to microtome for TEM after pyrolysis owing to their fragility, and the structure was partly destroyed and collapsed.

Figure 4a presents SAXS curves for the cured samples before pyrolysis. For $w_{PS} = 50$ %, at least six equally spaced intensity maxima were observed, the first located at ca. 0.014 Å^{-1}, indicating a highly ordered lamellar structure with a periodicity of ca. 45 nm. For $w_{PS} = 60$ % and 70 %, lamellar structures were observed with periods of ca. 42 and 39 nm, respectively. The structure of pure PS-*block*-P4VP could not be deduced from SAXS data, as the intensity maxima were too broad. TEM, however, shows a spherical structure. Also, for mixtures containing less than 50 % PS, the scattering intensity maxima become broadened and it is progressively more difficult to assign the structure based on SAXS alone. In such cases, TEM proves to be more useful (see Fig. 3 for $w_{PS} = 40$ %, 30 %, and 20 %).

SAXS curves for the corresponding samples after pyrolysis are shown in Figure 4b. Even if not directly evident from Figures 4a,b, the intensity of the scattered radiation was

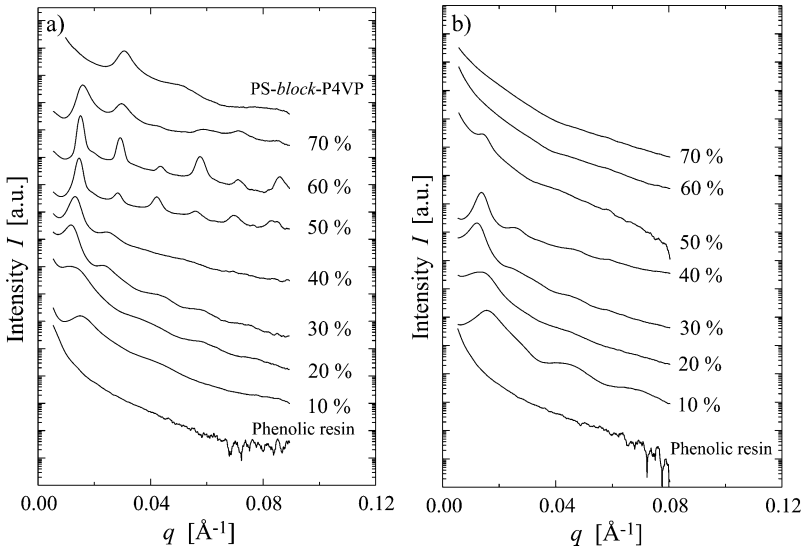

Figure 4. SAXS intensity patterns for PS-*block*-P4VP, phenolic resin and complexes before (a) and after (b) pyrolysis. The intensity has been Lorentz-corrected for lamellar (w_{PS} = 50–70 % before pyrolysis) and cylindrical structures (w_{PS} = 40 % before and after pyrolysis) by multiplying by q^2 and q, respectively. The weight fraction of PS is indicated (w_{PS}). The magnitude of the scattering vector is defined by $q = (4\pi/\lambda)\sin\theta$, where 2θ is the scattering angle, and λ = 1.54 Å.

almost two decades higher in the pyrolyzed samples than in the unpyrolyzed samples. This could be explained by the increased electron-density difference between the self-assembled domains, as caused by the selective degradation in pyrolysis. For samples with $w_{PS} < 50$ %, the scattering-peak positions did not change significantly as a result of pyrolysis. The fact that higher-order reflections could not be distinguished more clearly after pyrolysis, could result from increased local variations of periodicities when chemical bonds are broken and new ones are formed during pyrolysis. For w_{PS} = 50 %, the well-defined lamellar structure observed prior to pyrolysis is totally lost and the faint peak is shifted to a larger value of scattering vector. This indicates that the lamellar structure partly collapses during pyrolysis.

In Figure 5, Fourier-transform infrared (FTIR) spectra are presented for the samples before and after pyrolysis in the wavenumber range 2700–3700 cm^{-1}, which is characteristic for hydroxyl bands. Pure PS-*block*-P4VP (curve i) does not show peaks above 3200 cm^{-1}. All samples containing phenols had a peak at ca. 3430 cm^{-1} and a shoulder at ca. 3500 cm^{-1}, corresponding to the stretching bands of hydrogen-bonded and free phenolic OH groups, respectively. The stretching bands of the OH groups do not disappear under the selected pyrolysis conditions, indicating that significant number of the OH groups remain after pyrolysis. On the other hand, peaks from the block copolymer are significantly diminished during pyrolysis. This agrees with the increased electron-density contrast in TEM, and could be explained by significant removal of the block-copolymer component upon pyrolysis.

Surface areas were measured from selected samples using the Brunauer–Emmett–Teller (BET) method. The surface areas were 340 $m^2 g^{-1}$ for the cylindrical structure (w_{PS} = 40 %), 145 $m^2 g^{-1}$ for the worm-like structure (w_{PS} = 30 %), and 56 $m^2 g^{-1}$ for the lamellar structure (w_{PS} = 50 %). The low surface area of the lamellar structure probably results from the partial collapse of the well-defined structure during pyrolysis, which was also observed in SAXS and TEM. The surface areas for reference materials, i.e., cured but not pyrolyzed complexes and cured and pyrolyzed phenolic resin, and for the spherical structure (w_{PS} = 20 %), were below the resolution of the measurement system (< 5 $m^2 g^{-1}$), indicating that porosity is really gained by the removal of structure-forming agent from the block-copolymer template during pyrolysis.

It was expected that the porous structure and the hydroxyl groups of the phenolic matrix could lead to a faster absorption rate and chemical selectivity. The absorption properties of two dye model compounds, i.e., Methylene Blue hydrate (MB) and Rhodamine 6G (R-6G) dissolved in Milli-Q water (concentration less than 0.010 wt.-%), were studied using UV-vis spectroscopy (see Fig. 6). MB is expected to have a strong selective interaction resulting from the hydrogen bonding between its nitrogen-containing aromatic ring and phenol, whereas R-6G is likely to have weaker absorption, owing to less-selective interactions. In order to study the absorption properties, porous phenolic material (pyrolyzed PS-*block*-P4VP/phenolic resin complex with a cylindrical porous structure, w_{PS} = 40 %) and a reference sample (pyrolyzed phenolic resin, w_{PS} = 0 %) were immersed into the dye solutions. The amount of the dyes was quite arbitrarily se-

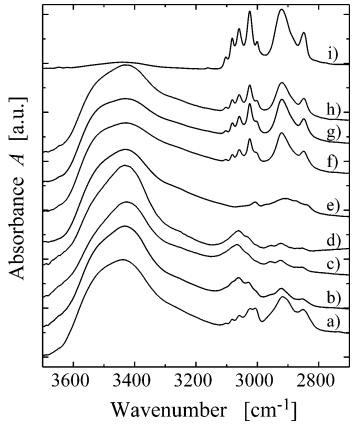

Figure 5. FTIR absorption bands in the range 2700–3700 cm^{-1} for the HMTA-cured PS-*block*-P4VP/phenolic resin complexes and PS-*block*-P4VP before and after pyrolysis. Samples are as follows; a) w_{PS} = 0 % after pyrolysis, b) w_{PS} = 30 % after pyrolysis, c) w_{PS} = 40 % after pyrolysis, d) w_{PS} = 50 % after pyrolysis, e) w_{PS} = 0 % before pyrolysis, f) w_{PS} = 30 % before pyrolysis, g) w_{PS} = 40 % before pyrolysis, h) w_{PS} = 50 % before pyrolysis, and i) pure PS-*block*-P4VP.

ADVANCED MATERIALS

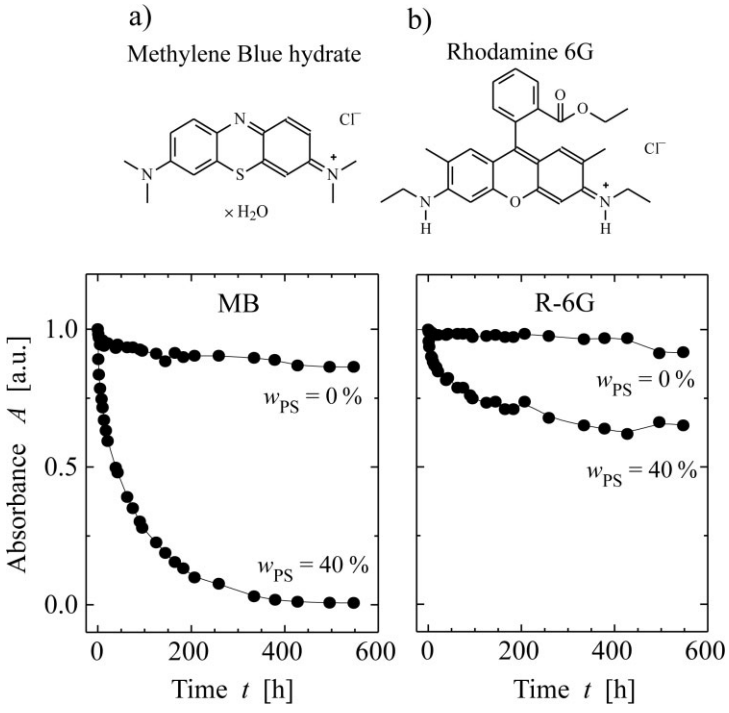

Figure 6. MB and R-6G concentrations in aqueous solutions as a function of time upon the addition of phenolic absorbents in the solutions. The denotation $w_{PS} = 40\,\%$ refers to HMTA-cured PS-*block*-P4VP/phenolic resin after pyrolysis, where the PS fraction in the mixture is 40 % leading to cylindrical pores. The denotion $w_{PS} = 0\,\%$ refers to the pyrolyzed phenolic resin without block copolymer, which has no porosity. a) Concentration of MB based on its characteristic UV-vis absorption at $\lambda = 665$ nm as a function of time. b) Concentration of R-6G based on its characteristic UV-vis absorption at $\lambda = 277$ nm as a function of time. Note that the absorbance depends on the concentration logarithmically.

lected so that the number of MB and R-6G molecules was 0.77 % of the nominal number of the hydroxyl groups of phenolic material. The characteristic UV-vis absorbance maxima (at 665 nm for MB and at 277 nm for R-6G) as a function of time are represented in Figure 6. In the case of MB, the nonporous reference material ($w_{PS} = 0\,\%$) absorbs a small amount of the dye from the solution during the first hours, after which the absorption rate levels off, and after ca. 200 h no significant changes in absorption are observed (Fig. 6a). The corresponding porous material ($w_{PS} = 40\,\%$) absorbs MB from solution much more rapidly and absorbance approaches zero near 400 h, indicating that most MB molecules have been absorbed from the solution. In contrast, in the case of R-6G, the reference material ($w_{PS} = 0\,\%$) absorbs only a very small amount of the dye from the solution (Fig. 6b), obviously as a result of weaker interactions. In the corresponding porous material, the absorption is fast within the first few first hours and then levels off to a relatively high absorbance level, indicating that a substantial amount of R-6G still remains in the solution. These results clearly support the expectations that the high absorption of MB in the pyrolyzed porous phenolic material results from the creation of porosity (as comparing the cases $w_{PS} = 0\,\%$ and 40 % for MB) and that the hydrogen bonding between the dye and the phenolic matter also plays an important role in absorption properties (as comparing the $w_{PS} = 0\,\%$ cases between MB and R-6G).

In summary, porous materials with a narrow distribution of pore sizes, high density of pores, large surface area per volume unit, and selective absorption properties can be easily prepared using templates of block copolymer and phenolic resin. When the block copolymer is removed by a controlled pyrolysis, porosity is obtained, with a high number of hydroxyl groups at the matrix and pore walls. We expect that such porous materials with a large number of functional groups could be useful for, e.g., sensors, separation materials, filters, and templates for catalysis.

Experimental

Materials: Poly(styrene)-*block*-poly(4-vinylpyridine) (PS-*block*-P4VP) diblock copolymer was provided by Polymer Source Ltd. and was used without further purification. The molecular weight of the PS and P4VP blocks and polydispersity were $M_{n,PS} = 40\,000$ g mol^{-1}, $M_{n,P4VP} = 5600$ g mol^{-1} and $M_w/M_n = 1.09$. Phenolic resin (Novolac) was supplied by Bayer Ltd. (Vulcadur RB) and was used without further purification. The crosslinking agent hexamethylenetetramine (HMTA) was acquired from Aldrich (99 + %) and tetrahydrofuran (THF) was provided by Riedel-de Haën (99.9 %).

Sample Preparation: The composition of complexes is described by the weight percent of PS in the final blend (w_{PS}). The phenolic resin/HMTA ratio in all the complexes was 88:12. Phenolic resin, HMTA, and PS-*block*-P4VP were dissolved in THF separately until the solutions were visually homogenous. The solutions were combined and the mixtures were stirred for one day at room temperature. THF was slowly evaporated at room temperature and thereafter the samples were vacuum dried at 30 °C for one day. Curing of the samples was performed using the following temperature profile: 100 °C for 2 h, 150 °C for 2 h, and finally 190 °C for 2 h. Samples were prepared with different weight fractions of PS, i.e., $w_{PS} = 0$, 10 %, 20 %, 30 %, 40 %, 50 %, 60 %, and 70 %. Pyrolysis of crosslinked samples was performed by heating a sample from room temperature up to 420 °C using the heating rate of 1 °C min^{-1} without a protective gas atmosphere. The form of the sample during pyrolysis (film with thickness of ca. 100 μm or powder) did not seem to have an effect on the resulting structures or porosity.

Thermogravimetric Analysis (TGA): Proper pyrolysis conditions for the cured samples were determined using TGA. TGA curves were measured using Mettler–Toledo TG50 thermogravimeter with TC11 processor. Samples were heated from 40 to 600 °C using a heating rate of 1 °C min^{-1} without a protective gas atmosphere.

Transmission Electron Microscopy (TEM): Crosslinked and pyrolyzed samples were embedded in epoxy and cured at 60 °C overnight. Thin sections (50–100 nm) were cut using Leica Ultracut UCT ultramicrotome and a diamond knife at room temperature. No staining was performed for the microtomed sections. Bright-field TEM was performed on a Tecnai 12 transmission electron microscope operating at an accelerating voltage of 120 kV.

Small-Angle X-Ray Scattering (SAXS): The SAXS measurements were performed at the Dutch–Belgian beamline (BM26B) of European Synchrotron Radiation Facility in Grenoble, using a beam of 10 keV. The crosslinked and pyrolyzed samples were pressed between two polyimide films. The SAXS data were collected with a two-dimensional multiwire proportional counter at a distance of

8.0 m from the sample. A description of the beamline is given elsewhere [46].

Fourier-Transform Infrared (FTIR) Spectroscopy: FTIR spectroscopy was used to study the phenolic hydroxyl groups in the samples. All IR spectra were obtained using a Nicolet Magna 750 FTIR spectrometer at room temperature. A minimum of 64 scans was averaged at a resolution of 2 cm^{-1}. The samples were grounded with potassium bromide crystals and pressed into pellets. The samples were dried in vacuum oven at 30 °C for 24 h before measurements.

Surface-Area Measurement: The surface area was determined with Micromeritics Flow-Sorb 2300 II analyzer using a single-point Brunauer–Emmett–Teller (BET) method at the temperature of liquid nitrogen ($P/P_0 = 0.30$). The samples were degassed (under nitrogen/helium flow) at 200 °C for 30 min before the measurement.

UV-Vis Spectroscopy: Absorption properties of the pyrolyzed phenolic materials were studied as a function of time using two low molecular weight dyes, i.e., Methylene Blue hydrate (MB) (Fluka, 97 %) and Rhodamine 6G (R-6G) (Fluka), dissolved in deionized (Milli-Q) water. The specular UV-vis spectra were measured using a Perkin–Elmer Lambda 950 spectrophotometer in the wavelength range of 250–900 nm. The samples for UV-vis measurements were prepared as follows. First, MB and R-6G were dissolved in Milli-Q water at concentration less than 0.010 wt.-%. Thereafter, the porous phenolic material (cylindrical structure, $w_{PS} = 40$ %) and reference sample ($w_{PS} = 0$ %) were immersed into the solutions (pyrolyzed films were grounded using a mortar). The amount of the materials was selected so that the number of MB and R-6G molecules was 0.77 % of the nominal moles of the hydroxyl groups of phenolic material.

Received: July 12, 2004
Final version: June 24, 2005
Published online: December 8, 2005

Note Added in Proof: After submission of this article, we became aware of another article submitted at the same time on a closely related topic: C. Liang, K. Hong, G. A. Guiochon, J. W. Mays, S. Dai, *Angew. Chem. Int. Ed.* **2004**, *43*, 5785.

[1] U. Beginn, *Adv. Mater.* **1998**, *10*, 1391.
[2] S. R. Batten, R. Robson, *Angew. Chem. Int. Ed.* **1998**, *37*, 1460.
[3] A. Nangia, *Curr. Opin. Solid State Mater. Sci.* **2001**, *5*, 115.
[4] C. R. Martin, *Chem. Mater.* **1996**, *8*, 1739.
[5] C. Jérôme, S. Demoustier-Champagne, R. Legras, R. Jérôme, *Chem. Eur. J.* **2000**, *6*, 3089.
[6] C. R. Martin, M. Nishizawa, K. Jirage, M. Kang, S. B. Lee, *Adv. Mater.* **2001**, *13*, 1351.
[7] C. T. Kresge, M. E. Leonowicz, W. J. Roth, J. C. Vartuli, J. S. Beck, *Nature* **1992**, *359*, 710.
[8] A. Monnier, F. Schüth, Q. Huo, D. Kumar, D. Margolese, R. S. Maxwell, G. D. Stucky, M. Krishnamurty, P. Petroff, A. Firouzi, M. Janicke, B. F. Chmelka, *Science* **1993**, *261*, 1299.
[9] Q. Huo, D. I. Margolese, U. Ciesla, P. Feng, T. E. Gier, P. Sieger, R. Leon, P. M. Petroff, F. Schüth, G. D. Stucky, *Nature* **1994**, *368*, 317.
[10] U. Ciesla, F. Schüth, *Micropor. Mesopor. Mater.* **1999**, *27*, 131.
[11] V. A. Russell, M. D. Ward, *Chem. Mater.* **1996**, *8*, 1654.
[12] V. A. Russell, C. C. Evans, W. Li, M. D. Ward, *Science* **1997**, *276*, 575.
[13] H. Gudbjartson, K. Biradha, K. M. Poirier, M. J. Zaworotko, *J. Am. Chem. Soc.* **1999**, *121*, 2599.
[14] S. S.-Y. Chui, S. M.-F. Lo, J. P. H. Charmant, A. G. Orpen, I. D. Williams, *Science* **1999**, *283*, 1148.
[15] T. Müller, J. Hulliger, W. Seichter, E. Weber, T. Weber, M. Wübbenhorst, *Chem. Eur. J.* **2000**, *6*, 54.
[16] J. Liu, G. E. Fryxell, S. Mattigod, T. S. Zemanian, Y. Shin, L.-Q. Wang, *Stud. Surf. Sci. Catal.* **2000**, *129*, 729.
[17] J. S. Seo, D. Whang, H. Lee, S. I. Jun, J. Oh, Y. J. Jeon, K. Kim, *Nature* **2000**, *404*, 982.
[18] D. G. Kurth, K. M. Fromm, J.-M. Lehn, *Eur. J. Inorg. Chem.* **2001**, *6*, 1523.
[19] C.-Y. Su, X.-P. Yang, B.-S. Kang, T. C. W. Mak, *Angew. Chem. Int. Ed.* **2001**, *40*, 1725.
[20] P. H. Dinolfo, J. T. Hupp, *Chem. Mater.* **2001**, *13*, 3113.
[21] M. Templin, A. Franck, A. Du Chesne, H. Leist, Y. Zhang, R. Ulrich, V. Schädler, U. Wiesner, *Science* **1997**, *278*, 1795.
[22] C. G. Göltner, S. Henke, M. C. Weissenberger, M. Antonietti, *Angew. Chem. Int. Ed.* **1998**, *37*, 613.
[23] P. F. W. Simon, R. Ulrich, H. W. Spiess, U. Wiesner, *Chem. Mater.* **2001**, *13*, 3464.
[24] M. Bognitzki, H. Hou, M. Ishaque, T. Frese, M. Hellwig, C. Schwarte, A. Schaper, J. H. Wendorff, A. Greiner, *Adv. Mater.* **2000**, *12*, 637.
[25] T. Thurn-Albrecht, J. Schotter, G. A. Kästle, N. Emley, T. Shibauchi, L. Krusin-Elbaum, K. Guarini, C. T. Black, M. T. Tuominen, T. P. Russell, *Science* **2000**, *290*, 2126.
[26] T. Xu, H.-C. Kim, J. DeRouchey, C. Seney, C. Levesque, P. Martin, C. M. Stafford, T. P. Russell, *Polymer* **2001**, *42*, 9091.
[27] S. A. Jenekhe, X. L. Chen, *Science* **1999**, *283*, 372.
[28] G. Widawski, M. Rawiso, B. Francois, *Nature* **1994**, *369*, 387.
[29] B. Francois, O. Pitois, J. Francois, *Adv. Mater.* **1995**, *7*, 1041.
[30] S. A. Miller, E. Kim, D. H. Gray, D. L. Gin, *Angew. Chem. Int. Ed.* **1999**, *38*, 3022.
[31] U. Beginn, G. Zipp, M. Möller, *Adv. Mater.* **2000**, *12*, 510.
[32] U. Beginn, G. Zipp, A. Mourran, P. Walther, M. Möller, *Adv. Mater.* **2000**, *12*, 513.
[33] H.-K. Lee, H. Lee, Y. H. Ko, Y. J. Chang, N.-K. Oh, W.-C. Zin, K. Kim, *Angew. Chem. Int. Ed.* **2001**, *40*, 2669.
[34] C. J. Hawker, J. L. Hedrick, R. D. Miller, W. Volksen, *MRS Bull.* **2000**, *25*, 54.
[35] R. Mäki-Ontto, K. de Moel, W. de Odorico, J. Ruokolainen, M. Stamm, G. ten Brinke, O. Ikkala, *Adv. Mater.* **2001**, *13*, 117.
[36] S. Valkama, T. Ruotsalainen, H. Kosonen, J. Ruokolainen, M. Torkkeli, R. Serimaa, G. Ten Brinke, O. Ikkala, *Macromolecules* **2003**, *36*, 3986.
[37] V. Percec, A. E. Dulcey, V. S. K. Balagurusamy, Y. Miura, J. Smidrkal, M. Peterca, S. Nummelin, U. Edlund, S. D. Hudson, P. A. Heiney, H. Duan, S. N. Magonov, S. A. Vinogradov, *Nature* **2004**, *430*, 764.
[38] J.-M. Lehn, *Supramolecular Chemistry*, VCH, Weinheim, Germany, **1995**.
[39] F. S. Bates, G. H. Fredrickson, *Annu. Rev. Phys. Chem.* **1990**, *41*, 525.
[40] I. W. Hamley, *The Physics of Block Copolymers*, Oxford University Press, Oxford, UK **1998**.
[41] M. Muthukumar, C. K. Ober, E. L. Thomas, *Science* **1997**, *277*, 1225.
[42] J. Ruokolainen, R. Mäkinen, M. Torkkeli, T. Mäkelä, R. Serimaa, G. Ten Brinke, O. Ikkala, *Science* **1998**, *280*, 557.
[43] O. Ikkala, G. ten Brinke, *Chem. Commun.* **2004**, 2131.
[44] H. Kosonen, J. Ruokolainen, M. Torkkeli, R. Serimaa, P. Nyholm, O. Ikkala, *Macromol. Chem. Phys.* **2002**, *203*, 388.
[45] H. Kosonen, J. Ruokolainen, P. Nyholm, O. Ikkala, *Macromolecules* **2001**, *34*, 3046.
[46] W. Bras, *J. Macromol. Sci. Phys.* **1998**, *B37*, 557.